
UNIVERSAL SLEEP DECODER: ALIGNING AWAKE AND SLEEP NEURAL REPRESENTATION ACROSS SUBJECTS

Zhongtao Chen^{*,1}, Hui Zheng^{*,2,4}, Haiteng Wang¹,
 Jianyang Zhou^{3,4}, Lin Zheng⁴, Yunzhe Liu^{†,1,4}

¹Beijing Normal University, ²Peking University,

³Capital Medical University, ⁴Chinese Institute for Brain Research

*Equal contribution, †yunzhe.liu@bnu.edu.cn

ABSTRACT

Decoding memory content from brain activity during sleep has long been a goal in neuroscience. While spontaneous reactivation of memories during sleep in rodents is known to support memory consolidation and offline learning, capturing memory replay in humans is challenging due to the absence of well-annotated sleep datasets and the substantial differences in neural patterns between wakefulness and sleep. To address these challenges, we designed a novel cognitive neuroscience experiment and collected a comprehensive, well-annotated electroencephalography (EEG) dataset from 134 subjects during both wakefulness and sleep. Leveraging this benchmark dataset, we developed the Universal Sleep Decoder (USD) to align neural representations between wakefulness and sleep across subjects and a real-time staging model comparable to offline staging algorithms. Our model achieves up to 23.00% and 21.15% offline, as well as 22.6% and 20.4% real-time top-1 zero-shot real-time decoding accuracy on unseen subjects for N2/3 stage and REM stage, which is much higher than the decoding performances using individual sleep data. Furthermore, fine-tuning USD on test subjects enhances decoding accuracy to 29.20% and 30.47% offline, as well as 27.9% and 29.4% real-time top-1 accuracy, a substantial improvement over the baseline chance of 6.7%. Model comparison and ablation analyses reveal that our design choices, including the use of (i) an additional contrastive objective to integrate awake and sleep neural signals and (ii) a shared encoder to enhance the alignment of awake and sleep neural signals, significantly contribute to these performances. Collectively, our findings and methodologies represent a significant advancement in the field of sleep decoding.

1 INTRODUCTION

Sleep plays a fundamental role in memory consolidation (Klinzing et al., 2019; Brodt et al., 2023). Past memories are known to reactivate during sleep, especially during the N2/3 stage of non-rapid eye-movement (NREM) sleep (Ngo & Staresina, 2022). In rodents, hippocampal cells have been found to replay their firing patterns during sleep, recapitulating awake experiences in a time-compressed order (Wilson & McNaughton, 1994; Skaggs & McNaughton, 1996). In humans, while direct cell recordings are rare, recording scalp electroencephalograms (EEG) during sleep is possible. Recent work on human sleep decoding has identified endogenous memory reactivation during the N2/3 stage of sleep, the extent of which was positively related to subsequent memory performance (Schreiner et al., 2021).

Despite the significance of sleep decoding in humans, attempts of this sort is scarce in both neuroscience and computer science community. This is because there does not exist a well-annotated sleep dataset that provides clear ground-truth information about which memory is activated and when during sleep. The population neural activity during wakefulness and sleep differ greatly, causing classifiers trained on awake periods to struggle when applied to sleep states (Liu et al., 2022). Generalizing neural representation across subjects is especially challenging during sleep due to the spontaneous nature of memory reactivation without timed neural responses.

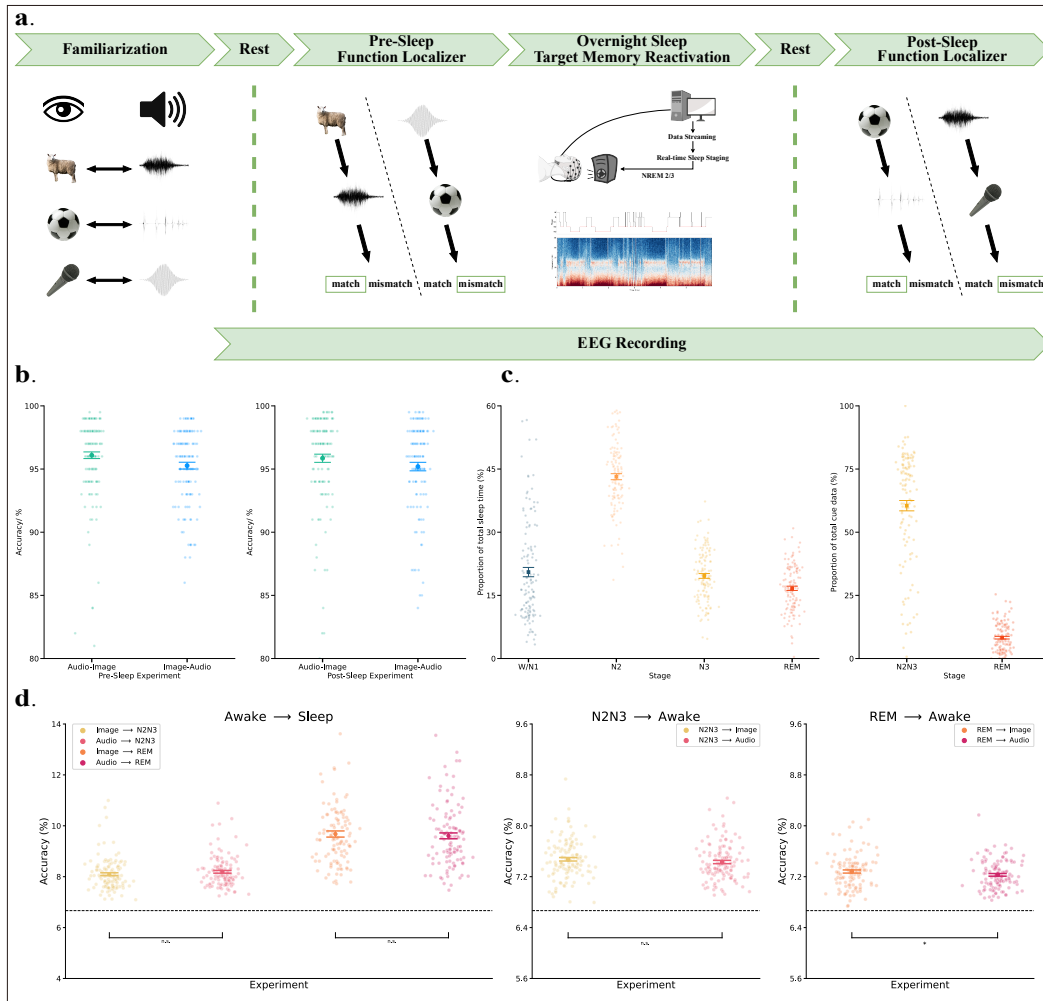


Figure 1: The experimental design for sleep decoding. (a) Before the experiment began, subjects were instructed to memorize 15 predefined pairs of pictures and sounds, each sharing the same semantic meaning; for example, a picture labeled "sheep" was paired with the sound of a sheep crying. After a rest period, subjects were exposed to 1000 trials, each of which contains one picture and one sound selected from these 15 pictures and 15 sounds (the picture and sound in one trial is not required to be paired), presented in either image-audio or audio-image order, and were asked to determine whether the pairs corresponded correctly. Subsequently, during overnight EEG recording, online, real-time sleep staging was performed. When subjects entered an NREM 2/3 sleep stage, auditory cues — randomly selected from the image-audio pairs — were played every 4-6 seconds. This step was crucial as it provided ground truth regarding which memory was activated and when. Following overnight sleep, subjects were again presented with 1000 image-audio pairs. Whole-brain 64-channel EEG recordings were collected throughout the experiment, during both sleep and wakefulness. More details can be found in Appendix.A.(b) During the pre-sleep and post-sleep function localizer stages, subjects were tasked with determining whether the presented image and audio cues were congruent. The two depicted images illustrate the accuracy of the experimental selections made by the subjects in both the pre-sleep and post-sleep function localizer stages, respectively.(c) The two graphs depict the proportions of various sleep states within the final collected sleep time and the distribution of these states within the audio stimulation data throughout the sleep process, respectively.(d) Performance on sleep EEG dataset of decoders trained on awake EEG dataset, and performance on awake EEG dataset of decoders trained on sleep EEG dataset. The decoder used here is a simple linear model: the Lasso GLM model, which is designed to confirm that there are common features that can be generalized and learned between the two different data domains.

To capture the content of neural reactivation in humans, we designed an innovative cognitive neuroscience experiment based on the classical targeted memory reactivation (TMR) paradigm (Rasch et al., 2007), see Fig.1a for more details. We employed a closed-loop stimulation system allowing for real-time, automatic sleep staging (Vallat & Walker, 2021a). When subjects reached the N2/3 stage of NREM sleep and REM sleep, auditory cues paired with visual objects were played every 4-6 seconds, with concurrent whole-brain EEG recordings. This approach provided precise timing and content of memory reactivation during sleep, facilitating the training of a neural decoder on these cued sleep intervals. Before and after sleep, subjects were asked to recall the auditory cue-visual object pairs, enabling the alignment of neural representations elicited by the same cue during both sleep and wakefulness. The high accuracy distributions shown in Fig.1b confirm that participants had formed correct and stable stimulus pair memories. This effort yielded a comprehensive dataset from 134 subjects, serving as the benchmark dataset for developing sleep decoders. Fig.1c shows the distribution of data that will be used in the subsequent training of the decoding and sleep staging models.

Based on this dataset, we introduce a Universal Sleep Decoder (USD) capable of decoding neural signals during NREM sleep and REM sleep, even on unseen subjects in a zero-shot manner. USD was pretrained in a supervised manner across a pool of subjects, learning subject-agnostic features and offering off-the-shelf decoding capabilities for new subjects. Given the challenges of sleep data collection, we also explored the potential to enhance sleep decoding performance by integrating relatively abundant awake task data. In the anticipation of the experimental design, it is expected that memories elicited via the same acoustic stimuli contain the same semantic information within their respective neural representations. Consequently, the wakefulness data are envisioned to facilitate the sleep decoding. Fig.1d substantiates the migratory dynamic existing between the two modalities through the training of a straightforward linear model, thereby enabling the feasibility of multimodal modeling. To encourage USD to learn domain-agnostic features, we incorporated a contrastive loss to align the neural representations elicited by the same cue during both sleep and wakefulness. With these design choices, USD achieves up to 22.6% and 20.4% top-1 zero-shot real-time decoding accuracy on unseen subjects for N2/3 stage and REM stage, which is much higher than the decoding performances using individual sleep data. Furthermore, fine-tuning USD on test subjects enhances real-time decoding accuracy to 27.9% and 29.4% top-1 accuracy, a notable improvement over the baseline chance of 6.7%. Overall, USD provides a powerful tool for manipulating memory reactivation in real time during sleep.

It is noteworthy that the proposed USD can also be effectively applied to other types of brain recordings with high temporal resolution, e.g., magnetoencephalography (MEG) or stereo-electroencephalography (sEEG). Our contributions are:

1. Establishing a well-annotated sleep dataset in humans, with ground truth regarding which memory was activated and when.
2. Showing that neural activity during wakefulness shares representations with sleep and aligning these can enhance the efficacy of sleep decoding.
3. The Universal Sleep Decoder (USD), a reusable, off-the-shelf, subject-agnostic real-time decoding model, offering a degree of zero-shot capability across subjects and can further improve performance through fine-tuning, establishing a new standard in sleep decoding methodologies.

2 RELATED WORK

2.1 SLEEP DECODING

During sleep, particularly during NREM sleep, humans are largely unconscious, and neural reactivation occurs spontaneously (Siclari et al., 2017; Schönauer et al., 2017). Consequently, gathering a well-annotated dataset that offers precise timing and content of neural reactivation during sleep is challenging, posing a significant hurdle in sleep decoding research. To address this challenge, some studies have attempted to extract memory reactivation content by soliciting reports from subjects either after they awaken or during their lucid dreaming (Horikawa et al., 2013; Siclari et al., 2017; Konkoly et al., 2021; Dresler et al., 2012). However, the data obtained is far less than what is

required to train the model, resulting in the current sleep decoder being trained on data from wakeful periods (Horikawa et al., 2013). Furthermore, this approach is limited solely to the REM sleep stage, where neural representation resembles that of wakefulness. Considering the neural patterns during NREM sleep—a period associated with memory replay—these exhibit even greater differences from those observed during wakefulness, making the memory decoding substantially more intricate. Consequently, this approach is unsuitable for decoding during NREM sleep.

Other studies in this field directly ignore the fact that the subjects are asleep (Türker et al., 2022). Sleep has classically been considered as a time when we are disconnected from the world, with significantly reduced (or absent) reactivity to external stimuli. However, several studies in recent years indicate that sleepers can process external stimuli at different levels of cognitive representation, encompassing semantic and decision-making stages, rather than merely at the level of low-level sensory processing (Strauss et al., 2015; Issa & Wang, 2011; Kouider et al., 2014). Furthermore, learning-related sensory cues presented during sleep positively impact subsequent recall of cue-related material upon awakening (Rasch et al., 2007; Hu et al., 2020), which is commonly referred to as Target Memory Reactivation (TMR). We follow these studies to design our cognitive neuroscience experiment, see Appendix.A for more details.

2.2 CONTRASTIVE LEARNING

Recently, the field of unsupervised learning has grown rapidly with the powerful contrastive learning (Chen et al., 2020). Meanwhile, Khosla et al. (2020) extend the contrastive loss to the supervised setting, thus allowing the model to learn a more discriminative representation for the classes. Along with the recent development of large models (Baeviski et al., 2020; Radford et al., 2021), many studies exploit the similarity of neural representations between the human brain and large models to improve the performance of neural decoding (Défossez et al., 2022; Chen et al., 2023). However, these approaches often require the collection of a dataset with a considerable number of labels for a single subject, which is impossible for the experiment design of sleep decoding (Türker et al., 2022; Hu et al., 2020). Similar to the TMR experiment setup, our designed experiment only allows us to gather a dataset with few labels, primarily because of the limited number of image-audio pairs available during the familiarization stage (see Fig.1).

Given the scarcity of available sleep datasets, no previous study has attempted to use contrastive learning to bridge the gap between brain activities recorded during wakefulness and sleep (i.e., two domains, in terms of domain generalization (Wang et al., 2022a)). The most relevant studies to our work mainly come from the fields of computer vision (Kim et al., 2021; Wang et al., 2022b) and natural language processing (Peng et al., 2018). Similar to these studies, we employ contrastive learning to align the neural representations elicited by the same cue during both wakefulness and sleep, thereby facilitating the acquisition of domain-agnostic features. Besides, domain adversarial training (Ganin et al., 2016; Zhu et al., 2020) could potentially offer a more robust approach for acquiring domain-agnostic features. However, that approach is not extensively investigated within the scope of this work.

2.3 PRETRAIN-FINETUNE PARADIGM

The pretrain-finetune paradigm is widely used in computer vision (Krizhevsky et al., 2012; He et al., 2022) and natural language processing (Devlin et al., 2018). In the early stages of pretraining development, supervised pretraining approaches (Krizhevsky et al., 2012) often outperform unsupervised pretraining approaches (Zhang et al., 2016; Noroozi & Favaro, 2016; Pathak et al., 2016) and serve as a baseline to evaluate the effectiveness of unsupervised methods.

Limited by the amount of available EEG recordings, only a few studies explored unsupervised pretraining methods for EEG signals (Kostas et al., 2021; Bai et al., 2023; Li et al., 2022b). Recently, most of the studies seek supervised pretraining methods to integrate different subjects (Zhao et al., 2021; Sun et al., 2022), learning subject-agnostic features that are generalizable to new subjects. Since there are fewer publicly available EEG recordings during sleep compared to those during wakefulness, applying unsupervised pretraining methods for sleep decoding is still under exploration. Consequently, we adopt supervised pretraining methods to further improve the performance of sleep decoding.

3 METHOD

We first formalize the general task of sleep decoding. Then, we introduce the deep learning architecture, and motivate the use of shared encoder and contrastive loss for training. Next, we introduce the pretrain-finetune paradigm when training on multiple subjects. The above steps are the same for both offline and real-time decoding, and we conclude by presenting a real-time sleep staging model that is integral to switching from offline to real-time decoding.

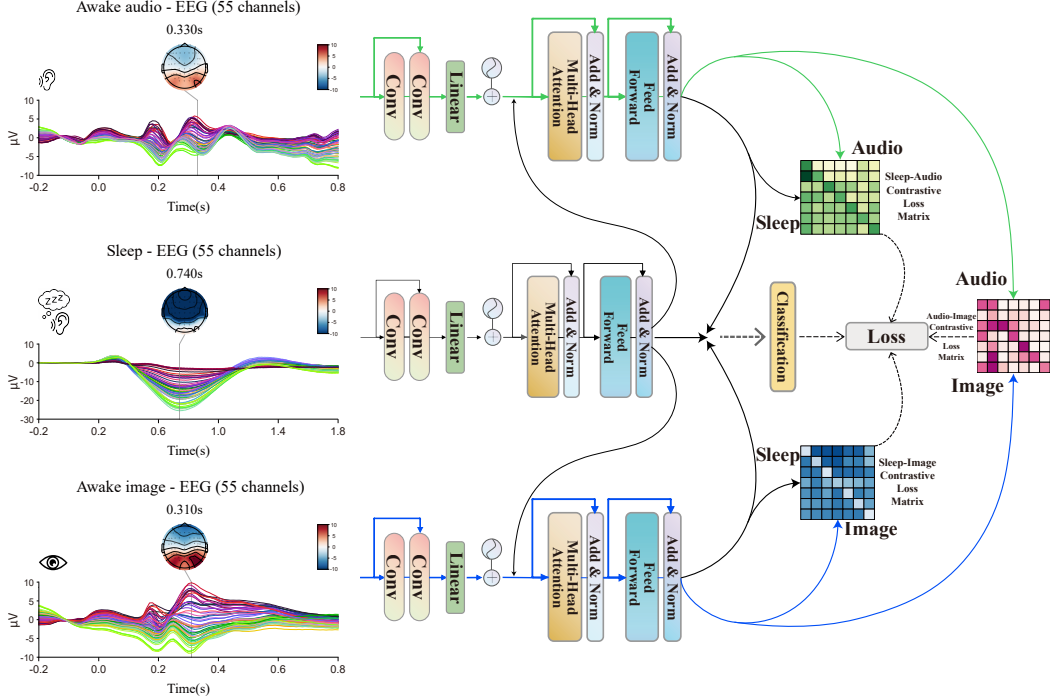


Figure 2: **Overview of Universal Sleep Decoder (USD)**. The model architecture consists of the neural encoder and the classification head. Contrastive loss is used to regularize the latent space, encouraging similarity among features sharing the same semantic class but coming from different domains (e.g. $\{\mathcal{D}_i^{img}, \mathcal{D}_i^{aud}, \mathcal{D}_i^{tmr}\}$) of the same subject i . Indeed, the awake EEG dataset and sleep EEG dataset can be perceived as disparate domains owing to the substantial disparity in their neural patterns. Through the utilization of the shared encoder approach and the integration of contrastive learning, the model adeptly aligns awake and sleep neural representations across subjects during the training process.

3.1 PRELIMINARIES

Following our designed cognitive experiment paradigm (see Fig.1), we recorded three different kinds (i.e., image-evoked, audio-evoked, and TMR-related) of EEG signals from each subject. Note that we refer to audio-evoked EEG signals during sleep as TMR-related, instead of TMR-evoked, as our experiment differs from the TMR paradigm. Different kinds of EEG signals can be viewed as different domains due to the large gap in their neural patterns, especially between awake and sleep EEG signals (Schönauer et al., 2017). As they share the same semantic classes, we define a pair-wise dataset format $\mathcal{D} = \{(x_n, y_n)\}_{n=1}^N$ and its corresponding single EEG data format $\mathcal{X} = \{x_n\}_{n=1}^N$, where $x \in \mathbb{R}^{C \times T}$ is the EEG signal, and $y \in \{1, \dots, K\}$ is a label indicating the index of semantic class in the dataset, stored in the form of one-hot encoding. C and T represent the channel dimension and the number of time steps respectively, while K is the number of semantic classes and N is the number of samples. Based on this definition, for each subject, we have datasets $(\mathcal{D}^{img}, \mathcal{D}^{aud}, \mathcal{D}^{tmr})$, which represent image-evoked, audio-evoked, and TMR-related EEG dataset respectively.

The goal of this work is to build a Universal Sleep Decoder (USD) based on the entire dataset $\{(\mathcal{D}_s^{img}, \mathcal{D}_s^{aud}, \mathcal{D}_s^{tmr})\}_{s \in \mathcal{S}}$, with \mathcal{S} the set of subjects, believing that the incorporation of datasets from various subjects, coupled with (resource-rich) awake EEG signals $(\mathcal{X}^{img}, \mathcal{X}^{aud})$ together is beneficial for learning generalizable and discriminative representations of (resource-poor) sleep EEG signals \mathcal{X}^{tmr} (Baltrušaitis et al., 2018; Wang et al., 2022a).

3.2 ARCHITECTURE

A general decoder framework commonly consists of a neural encoder f_{enc} and a classification head f_{cls} , see Fig.2. The neural encoder f_{enc} maps the neural signal x to the latent feature $z \in \mathbb{R}^F$, with F the latent dimension. And the classification head f_{cls} maps the latent feature z to the label distribution \hat{y} . In this work, we implement a CNN and transformer-based neural encoder that has different configurations in NREM 2/3 sleep and REM sleep. More details can be found in Appendix.C.

How semantic classes are represented in the brain during sleep is largely unknown (Türker et al., 2022). We can train the sleep decoder in a supervised manner, similar to what we commonly do when decoding awake neural signals. Specifically, when the neural encoder f_{enc} and the classification head f_{cls} belong to a parameterized family of models such as deep neural network, they can be trained with a classification loss $\mathcal{L}_{cls}(y, \hat{y})$ (e.g. the Cross-Entropy Error),

$$\min_{f_{enc}, f_{cls}} \sum_{x, y} \mathcal{L}_{cls}(y, f_{cls}(f_{enc}(x))). \quad (1)$$

Empirically, we observed that directly applying this supervised decoding approach to sleep data faces several challenges:

1. the limited number of annotated samples within each subject.
2. the noisy signals, and the potentially unreliable labels (e.g. not all audio cues induce the desired cognitive processes (Türker et al., 2022)).

These challenges lead to significant overfitting issues. In comparison, awake datasets $(\mathcal{D}^{img}, \mathcal{D}^{aud})$ are more resource-rich, as we can obtain more samples with reliable annotations easily. As mentioned before, these datasets can be seen as different domains due to the large gap in their neural patterns. To encourage the similarity among features sharing the same semantic class but coming from different domains, introduce two special structural designs: a shared encoder and an additional contrast loss in the training target.

The shared encoder in the structure is based on the Transformer, and the image EEG signals and audio EEG signals from the wakefulness data are input in the shared encoder with the sleep EEG signals, respectively, in order to ensure that richer and more effective semantic information can be extracted from the different modalities and help in the sleep decoding. Meanwhile, the existence of the shared encoder makes it possible to fine-tune the model using only the test subject’s wakefulness data, thus directly improving the accuracy of corresponding sleep decoding.

The additional contrast learning loss actually consists of three small components, the sleep EEG signals versus the awake image EEG signals, the sleep EEG signals versus the awake audio EEG signals and the awake image EEG signals versus the awake audio EEG signals:

$$\mathcal{L}_{total} = \mathcal{L}_{cls} + \lambda \mathcal{L}_{contra}, \quad (2)$$

where λ is a weighting coefficient to balance the losses. To introduce the label information, we follow the setting of supervised contrastive loss (Khosla et al., 2020). To balance the proportion of sleep data during training, we oversample sleep data for each training batch, ensuring the model encounters both awake and sleep data equally.

Here, we take image-evoked dataset \mathcal{D}^{img} and TMR-related dataset \mathcal{D}^{tmr} for example. For each batch, we draw equal (i.e., $\frac{|\mathcal{B}|}{2}$) sample pairs from these datasets respectively, shuffle them, and then reassemble them into a new dataset. Thus, we have $\mathcal{B} = \{(x_i, y_i)\}_{i=1}^{|\mathcal{B}|}$, while each item (x_i, y_i) is from either \mathcal{D}^{img} or \mathcal{D}^{tmr} . Then, each neural signal x_i is mapped to the latent feature z_i through

the same neural encoder f_{enc} . The contrastive loss is computed by:

$$\mathcal{L}_{contra} = - \sum_{i \in \{1, \dots, |\mathcal{B}|\}} \frac{1}{|\mathcal{P}(i)|} \sum_{k \in \mathcal{P}(i)} \log \frac{e^{\langle z_i, z_k \rangle}}{\sum_{j \in \mathcal{A}(i)} e^{\langle z_i, z_j \rangle}} \quad (3)$$

where $\mathcal{A}(i) = \{1, \dots, |\mathcal{B}|\} \setminus \{i\}$, $\mathcal{P}(i) = \{k | k \in \mathcal{A}(i), y_k = y_i\}$, and $\langle \cdot, \cdot \rangle$ the inner product.

3.3 PRETRAIN-FINETUNE PIPELINE

Our method consists primarily of two stages: the pretraining stage and the finetuning stage. During the pretraining stage (see Fig.2), we leave one subject out, e.g. subject i . Then, we use the datasets from the rest subjects to format the training dataset $\mathcal{D}_{train} = \{(\mathcal{D}_s^{img}, \mathcal{D}_s^{aud}, \mathcal{D}_s^{tmr})\}_{s \in \mathcal{S} \setminus \{i\}}$. Following the previous training procedure, we get a pretrained model for that subject. During the finetuning stage, the pretrained model can either be directly evaluated on the sleep data of the test subject, i.e., \mathcal{D}_i^{tmr} , or be fine-tuned on part of that dataset before evaluation. Most of the time, the zero-shot setting is preferred because sleep data is usually difficult to collect and the amount of sleep data for each subject is extremely limited. While fine-tuning can lead to improved performance, it also demands more computing resources. We explore both use cases in this work.

Since the self-similarity operation in the Transformer provides a modeling method that is more adaptive and robust than the convolution operation (Hoyer et al., 2022), the Transformer-based neural encoder is more suitable for learning subject-agnostic features. Hence, we primarily utilize the transformer as the core element of the neural encoder, with the CNN serving as the initial stage to roughly extract semantic information across various temporal scales. Recognizing the limited availability of REM sleep data, we introduce a "Subject layer" at the conclusion of the CNN encoder for processing sober data within the REM model. This adaptation aims to facilitate semantic information extraction in scenarios characterized by a wide diversity of data but limited per capita data volume. The "Subject Layer," designed to capitalize on inter-subject variability more effectively, learns a distinct matrix $M_s \in \mathbb{R}^{D \times D}$ for each subject $s \in \mathcal{S}$. (Défossez et al., 2022; Haxby et al., 2020).

3.4 REAL-TIME SLEEP STAGING MODEL

As depicted in Fig3, for optimal staging efficacy, the model harnesses data from three channels (EEG, EOG, EMG) as inputs and conducts comprehensive staging analysis through the tandem processing of CNN model blocks and LSTM model. The loss term of the model encompasses cross-entropy error and mean square error:

$$\mathcal{L}_{total} = \mathcal{L}_{cls} + \mathcal{L}_{mse}, \quad (4)$$

To compute the mean square error, we assigned the corresponding labeling values of the four sleep states (W/N1, N2, N3, and REM) as 0, 1, 2, and 3. This served as the basis for calculating the mean square error between the ground truth and the predicted labels.

4 EXPERIMENTS

In this section, we present results from three subsections: offline sleep decoding results, real-time sleep staging results, and real-time sleep decoding results. For the sleep decoding segment, we validated the three research hypotheses through ablation experiments and model comparisons:

1. The superiority of the thematic design of the Universal Sleep Decoder (USD) model and the effectiveness of applying comparative learning and a shared encoder compared to other models.
2. The inclusion of (resource-rich) wakefulness data can mitigate overfitting issues stemming from the noisy nature of sleep data.
3. Incorporating datasets from different subjects aids the model in acquiring subject-independent features, thereby ultimately enhancing performance.

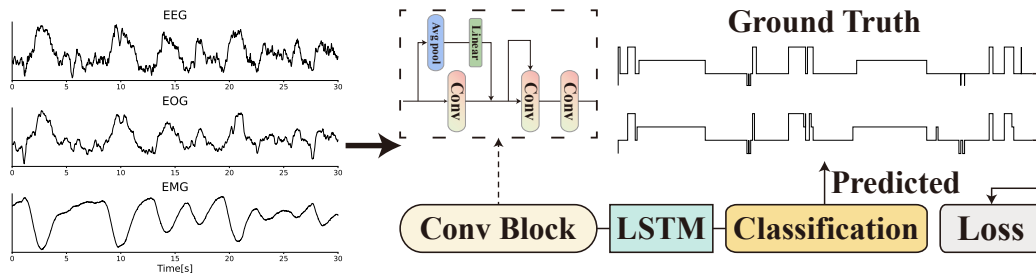


Figure 3: **Overview of Real-time Sleep Staging Model.** The model architecture comprises a CNN block, an LSTM network, and a classification head. To maximize staging efficacy, the model utilizes data from three channels (EEG-C3, EOG, EMG) as inputs. The loss function of the model incorporates both cross-entropy error and mean-square error terms. This combination aims to address the imbalance in the distribution of data volume across each stage in the sleep data, thereby enhancing the accuracy of sleep staging.

4.1 DATASETS

As mentioned before, humans are still able to receive and process external sensory stimuli during sleep, even at the semantic level. Therefore, following our designed experiment paradigm (see Fig. 1a), we can collect neural signals sharing the same semantic neural patterns during both wakefulness and sleep. Besides, the experiment paradigm also provides clear timing and content of memory reactivation during sleep. These two properties together render our dataset a foundational benchmark dataset to validate our research hypotheses. Given the absence of publicly available sleep datasets, we validate our model on the sleep dataset collected by ourselves.

In our dataset, non-invasive EEG recordings were collected during 5 sessions from 134 healthy subjects. Notably, the data for 122 subjects were collected in one laboratory, whereas the data for the remaining 12 subjects were gathered in a different laboratory. Approximately, 12 hours of data were recorded using a 64-channel EEG cap from each subject; see Appendix.A. All subjects share a common set of 15 semantic classes. Before the downstream analysis, we have dropped bad trials before the downstream analysis, see Appendix.B. For each subject, we get 2000 image-evoked EEG signals, 2000 audio-evoked EEG signals, and 1000 TMR-related EEG signals, all with well-balanced labels. Prior to training, the EEG signals underwent filtering within the frequency range of 0.1-50Hz, followed by resampling to 100Hz. Subsequently, the signals were epoched from -0.2s to 0.8s for awake EEG signals and from -0.2s to 1.8s for sleep EEG signals based on the onset of stimulus cues.

4.2 OFFLINE SLEEP DECODING RESULTS

To assess the first hypothesis, we implement four distinct decoding models. Initially, these models are trained without incorporating contrastive learning and wakefulness data. We compared the zero-shot accuracy of the four models to evaluate their performance. Subsequently, contrastive learning and shared encoders are gradually introduced into the encoders of the basic USD model. We assess the performance of these designs based on their corresponding zero-shot accuracy.

For testing the second hypothesis, we examine the fine-tuning and zero-shot decoding outcomes for the full model state. This evaluation includes scenarios where the model is trained solely using sleep data, as well as instances where both sleep and wakefulness data are utilized for training. By visually comparing the performance results of the same models under both the zero-shot training paradigm and the fine-tuning paradigm, we investigate the third hypothesis.

4.2.1 MODEL COMPARISON AND ABLATION EXPERIMENT

We commence with an introduction to the four models employed for comparison: the Logistic GLM model, the CNN-based model, the Transformer-based model, and our Universal Sleep Decoder

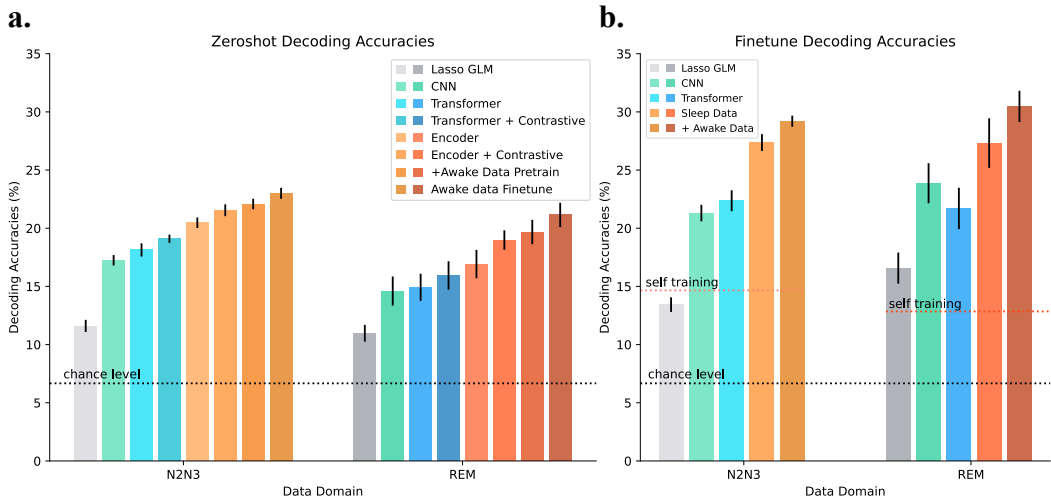


Figure 4: **Offline sleep decoding results.** (a). Zero-shot Decoding Performance on sleep dataset of decoders trained on sleep dataset or awake & sleep dataset. The average performance and standard error are illustrated in bar charts, with the decoding results for the NREM 2/3 state and the REM state displayed in two distinct sections of the graph. The highest average decoding accuracies achieved by the best-performing USD model are 23.00% and 21.15% for the NREM 2/3 state and REM state. (b). Fine-tune performance of decoders pretrained on sleep dataset or awake & sleep dataset. The highest average decoding accuracies achieved by the best-performing USD model are 29.20% and 30.47% for the NREM 2/3 state and REM state. It should be noted that in the awake & sleep pretrained model, the amount of fine-tuned data utilized is three times greater than that used in the sleep pretrained model. This is because each sleep data item is paired with an image data item and an audio data item, both randomly selected from the same subject’s wakefulness dataset. ”self training” refers to average performance of the model trained on one single test subject and tested on the same subject.

(USD) model. Logistic GLM follows the standard setup in neuroscience (Liu et al., 2021): we train and evaluate a time-specific classifier for each time point, then take the maximum accuracy among these classifiers. The CNN-based model comprises two basic convolutional layers, whereas the Transformer-based model consists of transformers with a depth of 8 and an attention head count of 6. For the USD model used for comparison, the ”Encoder” model for comparison corresponds only to the ”Sleep Encoder” part of the full model ; see Appendix.C for more details.

For the design of the ablation experiments, given that the encoder of the USD model is themed on the Transformer architecture, we introduced comparative learning to both the Transformer-based model and the USD’s ”Encoder” model. Subsequently, upon integrating comparative learning, we further incorporated the shared encoder to obtain the complete USD model; see Appendix.C for more details.

As mentioned before, the whole dataset comes from two different laboratories. According their sources, we split the set of subjects \mathcal{S} (containing 134 subjects) into two subsets: \mathcal{S}_1 (containing 122 subjects), and \mathcal{S}_2 (containing 12 subjects). During the pretraining stage, the datasets $\{(\mathcal{D}_s^{img}, \mathcal{D}_s^{aud}, \mathcal{D}_s^{tmr})\}_{s \in \mathcal{S}_1}$ from \mathcal{S}_1 are used for the supervised pretraining of USD. In total, there are approximately 240,000 image-evoked data, 240,000 audio-evoked data, 30,000 TMR-related REM sleep data and 120,000 TMR-related NREM 2/3 sleep data across 122 subjects for supervised pretraining USD. Then, the datasets $(\mathcal{D}_i^{img}, \mathcal{D}_i^{aud}, \mathcal{D}_i^{tmr})$ of subject $i \in \mathcal{S}_2$ are used for latter evaluation.

In the model comparison section, only sleep data is required for model training. However, in the ablation experiment section, which includes both the comparative learning and shared encoder components, the model needs to be trained using complete datasets containing both sleep and wakefulness data. Here, we pretrain models separately on sleep-only datasets (i.e., $\{\mathcal{D}_s^{tmr}\}_{s \in \mathcal{S}_1}$) and the

whole datasets (i.e., $\{\mathcal{D}_s^{img}, \mathcal{D}_s^{aud}, \mathcal{D}_s^{tmr}\}_{s \in \mathcal{S}_1}$), to further investigate the first hypothesis in the zero-shot decoding. Due to the limited computing resources, we only evaluate these experiments on the 12 subjects from \mathcal{S}_2 . Since the data of \mathcal{S}_1 and \mathcal{S}_2 comes from two different laboratories, the experiments can better validate the generalization ability of our model. The results for each subject are averaged across 5 seeds.

After the pretraining stage, we directly apply the pretrained model for sleep decoding on the held-out subject, one that the model has not previously encountered. We investigate the zero-shot ability of models and validate the superior performance of the USD model on NREM 2/3 sleep data and REM sleep data separately; see Fig.4a. It is evident that the decoding results of all models significantly surpass the chance level. This result aligns with prior research findings (Türker et al., 2022) — even during NREM sleep, the human brain still responds to external stimuli. Particularly, when utilizing only sleep data, it becomes apparent that the decoding accuracy of the USD’s ”Encoder” model notably exceeds that of the other three models. Upon further investigation, it becomes evident that the USD model consistently outperforms the Transformer-based model, even when incorporating comparative learning and utilizing all available data. Moreover, the inclusion of a shared encoder demonstrates a further enhancement in the model’s decoding capability. These findings clearly underscore the superiority of the encoder component within the USD model and underscore the necessity and significance of employing comparative learning and a shared encoder to enhance decoding performance.

4.2.2 IMPROVE SLEEP DECODING WITH AWAKE DATASET

We have demonstrated the potential for transfer learning, see Fig.1d, and through testing the previous hypothesis, we have also presented preliminary evidence suggesting that we can enhance sleep decoding performance by leveraging the awake dataset. In this section, we will delve more deeply into rationalizing the utilization of awake data to comprehensively improve sleep decoding performance.

For the USD model, the zero-shot accuracies for the NREM 2/3 state and the REM state averages at 21.55% and 18.99%, respectively, while the fine-tuning accuracies using only sleep data reaches 27.37% and 27.32%. Upon incorporating awake data and applying contrast learning and shared encoder during pretraining, we observe improvements in zero-shot accuracies to 22.08% and 19.68%, and in fine-tuning accuracies to 29.20% and 30.47% for the NREM 2/3 state and the REM state, respectively. Additionally, the inclusion of the shared encoder design facilitates partial fine-tuning of the model using the awake data of the test subjects, resulting in further enhancements in zero-shot accuracies to 23.00% and 21.15%. The substantial enhancement observed in both zero-shot and fine-tuning decoding results validates our hypothesis that wakefulness data can mitigate the sleep decoding overfitting issue and enhance decoding performance. This underscores the potential of leveraging rich wakefulness data to augment sleep decoding capabilities.

4.2.3 FINE-TUNE RESULT ON SLEEP DECODING

The fine-tuning process comes after the pretraining phase, in which we will fine-tune the pretrained model using data from the test subjects. For each dataset of test subject i , i.e., $\mathcal{D}_i^{img}, \mathcal{D}_i^{aud}, \mathcal{D}_i^{tmr}$, we split the dataset into training, validation, testing splits with a size roughly proportional to 80%, 10%, and 10%. We train each model with the training split for 200 epochs, and then evaluate its performance on validation and testing splits. We take the test accuracy according to the maximum validation accuracy as its performance and compute their average as their performance.

The fine-tuning results for both NREM 2/3 and REM state data are depicted in Fig.4b, with the results obtained by training and decoding the USD model using the same data division indicated by the dotted line labeled ”self-training”. It is evident that the fine-tuning results of the CNN-based model, Transformer-based model, and USD model after pretraining significantly surpass the ”self-training” result. Interestingly, even the Lasso GLM model, in the REM state, can achieve higher performance than the ”self-training” result. Moreover, in the REM state, the Lasso GLM model outperforms the ”self-training” result. Notably, the USD model fine-tuned with all the data exhibits substantially higher decoding performance than ”self-training” and significantly outperforms the other models, reaching a maximum of 29.20% in the NREM 2/3 state and 30.47% in the REM state. These findings reaffirm the previous hypotheses and demonstrate that models trained using the pretrain-finetune paradigm are motivated to learn more independent features unrelated to the

subject of study by incorporating datasets from different subjects, ultimately enhancing the decoding performance of the model on the original dataset.

4.3 REAL-TIME SLEEP STAGING RESULTS

Based on offline decoding, we embark on a quest to delve into real-time decoding, with the initial focus centers on the development of an efficient real-time sleep staging model.

Similar to the training process of the decoding model, we utilized sleep data from 122 subjects as the training set to pretrain the real-time sleep staging model. This pretraining was based on data from three channels (EEG-C3, EOG, EMG), and staging tests were conducted on the sleep data of 12 test subjects. To align with actual real-time sleep staging requirements, we set the input data time length to 30 seconds, with a sliding window applied every 3 seconds for subsequent staging. For the staging results of the real-time sleep model, we considered the initial 30-second staging results as the onset of the initial sleep state. Subsequently, based on this onset, we assigned the staging results after each sliding window to the corresponding sleep state within the 3-second time period.

As Yasa is considered the best-performing sleep staging algorithm in the offline state, it serves as a reference when manual staging results are unavailable. Consequently, our objective in training a real-time sleep staging model is to develop a model capable of staging performance comparable to Yasa. To evaluate the model training results, we selected one of the twelve test subjects and visually compared the staging results of the two staging methods with those of the ground truth. The offline staging results of Yasa achieve a consistency of 92.78% compared to the ground truth, while the real-time sleep staging model achieves a consistency of 94.41%; see Fig5a. Additionally, Fig5a displays the spectrogram of this subject below the hypnogram, This type of plot can be used to easily identify the overall sleep architecture. For example, periods with high power in frequencies below 5 Hz most likely indicate deep non-rapid eye movement (NREM) sleep (Vallat & Walker, 2021b).

For the conclusive staging outcomes, the performance of the real-time sleep staging model slightly outperforms that of the Yasa offline staging, with an average accuracy of 90.38% across the data of 12 test subjects. This accuracy is marginally higher compared to the average accuracy of 90.05% achieved by Yasa offline staging; see Fig5b. However, when using Yasa to simulate real-time decoding, given that Yasa requires a minimum input data length of 5 minutes (Vallat & Walker, 2021b), we adjust the data accordingly while maintaining the 3-second sliding window. Additionally, we preserve the selection of overall staging results in the same manner as our real-time staging model. Under these conditions, the average accuracy of the approximate real-time staging results of the Yasa model only reaches 63.86%, significantly lower than the performance of our real-time sleep staging model.

Next, we conduct a detailed examination of the classification performance of the real-time sleep staging model for each sleep stage ; see Fig5c. We observe an overall accuracy of 88.8% for the N3 sleep stage, 93.5% for the N2 sleep stage, and 92.9% for the REM sleep stage. For the remaining wakefulness and the N1 sleep stage, which we categorized together, the overall accuracy is 83.8%. The distribution of the staging results for each test subject, compared to the manual staging results, is illustrated in Fig5d. It is evident that the distribution of staging results of the real-time sleep staging model exhibits minimal deviation compared to the ground truth. Particularly, the difference in the distribution of the N3 sleep stage and the REM sleep stage is notably small. Upon comparison of the distribution of stable and migrated states, it becomes apparent that the disparity between the current distribution and the portion of the error arises from the fact that the current staging model recognizes some migrated sleep periods as stable states.

4.4 REAL-TIME SLEEP DECODING RESULTS

Having established a mature real-time sleep staging model, we further delve into the real-time sleep decoding model. In contrast to offline decoding, the primary challenge of real-time decoding lies not in the design of the model, but rather in the preprocessing of sleep data. Unlike offline decoding, where preprocessing occurs prior to analysis, real-time decoding relies on the real-time sleep staging results for data acquisition. Consequently, we streamline the preprocessing process to include filtering, downsampling, and re-referencing for each segment of data. This simplified preprocessing approach allows for efficient decoding of the preprocessed data in real-time.

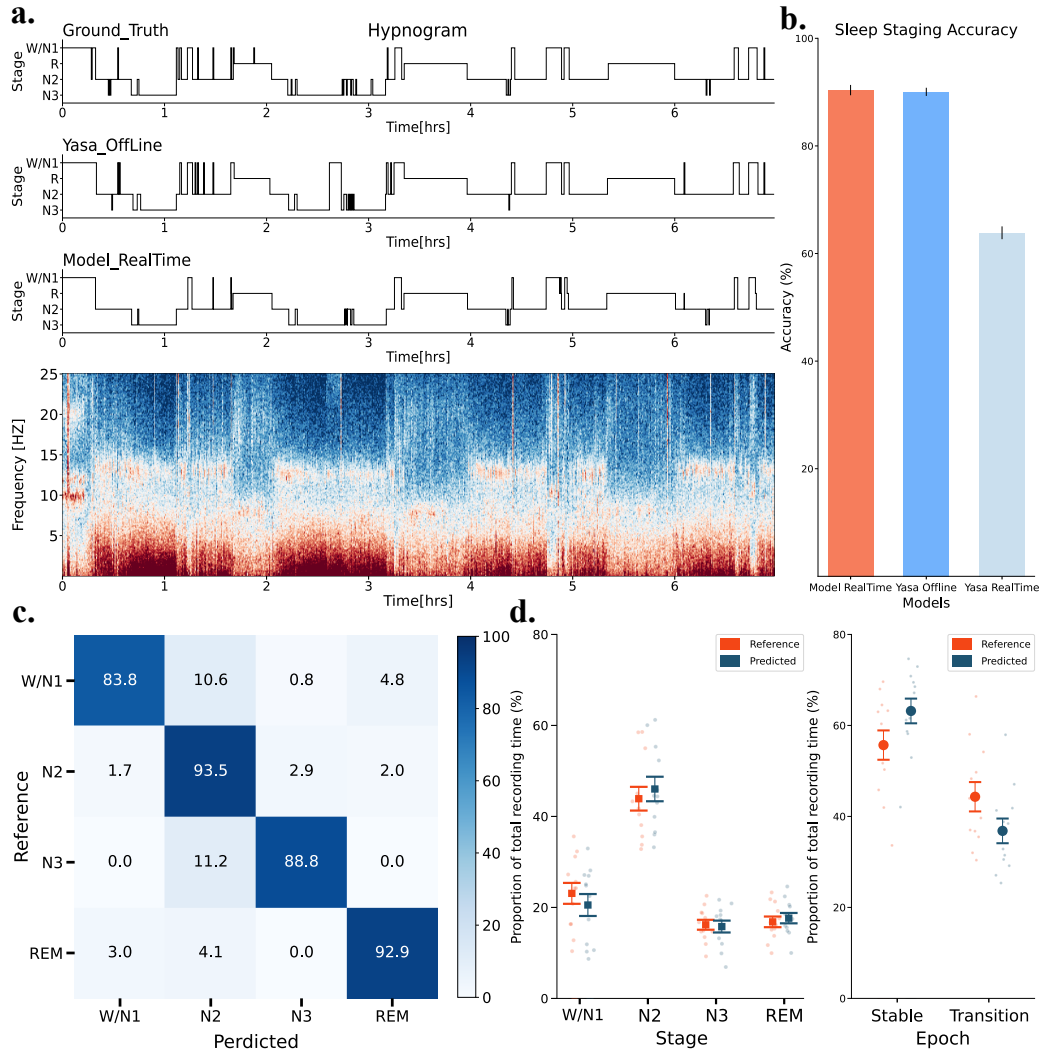


Figure 5: **Real-time sleep staging results (a).** Grounf-truth (= human-scored) and Yasa Offline and model real-time predicted hypnogram in one test subject. The agreement between the grounf-truth and yasa offline scoring is 92.78%. The agreement between the grounf-truth and model real-time predicted scoring is 94.41%. **(b).** Below the hypnogram is the corresponding full-night spectrogram of the central electroencephalogram (EEG) channel. Warmer colors indicate higher power in these frequencies. **(c).** Bar charts illustrating the accuracies of different model staging, along with the corresponding error bars. **(d).** Confusion matrix. The diagonal elements represent the percentage of epochs that are correctly classified by the real-time model (also known as sensitivity or recall), whereas the off-diagonal elements show the percentage of epochs that are mislabeled by the real-time model. **(e).** Duration of each stage, and Duration of stable state and transition state in the human (red) and real-time model scoring (blue), calculated for each unique testing night and expressed as a proportion of the total duration of the polysomnography (PSG) recording. An epoch is considered around a transition if a stage transition, as defined by the human scoring, is present within the 3 min around the epoch (1.5 min before, 1.5 min after).(Vallat & Walker, 2021b)

When considering the choice of decoding model for real-time applications, the superiority of the current model’s structure and its improved decoding performance, facilitated by the unique contrast learning and shared encoder, has been demonstrated in offline decoding results. Given the robustness and stability typically associated with deep learning models, we opt to adopt the entire model structure for real-time sleep decoding. We reprocess the original data according to the real-time pre-

processing paradigm for both training and testing, utilizing the corresponding real-time preprocessed test data. The results obtained are depicted in Fig6.

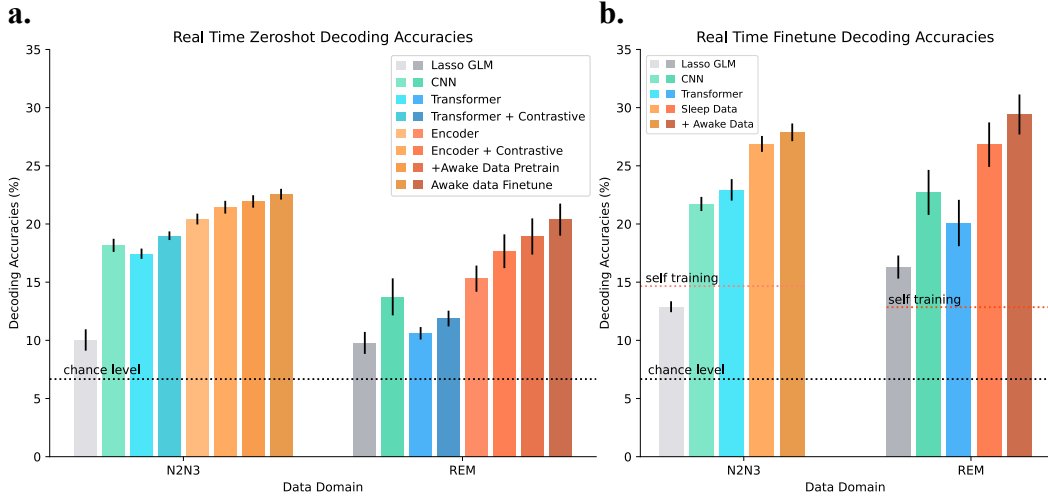


Figure 6: **Real-time sleep decoding results** It is observed that the decoding performance of all models in real-time sleep decoding exhibits some degradation compared to offline decoding. Among these models, the real-time decoding results of the USD model demonstrate only a slight degradation compared to offline decoding, maintaining significantly higher decoding accuracy than all other models. **(a)**. In zero-shot decoding, the highest average decoding accuracies achieved by the USD model are 22.56% and 20.38% for the NREM 2/3 state and REM state. This represents a decrease of 0.44% and 0.77%, compared with offline decoding. **(b)**. In fine-tune decoding, the highest average decoding accuracies achieved by the USD model are 27.88% and 29.41% for the NREM 2/3 state and the REM state. This reflects a decrease of 1.32% and 1.06%, compared to offline decoding.

Ultimately, after refining the tuning data preprocessing steps and retraining, we successfully developed a USD model that is proficient for real-time decoding tasks. The USD model for real-time decoding can accomplish decoding within 100-200 ms, with a performance degradation of no more than 1.5% compared to the offline decoding model. For the zero-shot decoding task, the real-time decoded USD model achieves the highest average decoding accuracies of 22.56% and 20.38% for NREM 2/3 and REM states, respectively. Moreover, the average decoding accuracies can be improved to 27.88% and 29.41% after fine-tuning.

5 CONCLUSION & LIMITATIONS

In this study, we introduce the Universal Sleep Decoder (USD), a model designed to align awake and sleep neural representations across subjects. This alignment creates representations that are both subject-agnostic and domain-agnostic, significantly enhancing the accuracy and data-efficiency of sleep decoding, even on unseen subjects. This advancement is crucial in neuroscience, a field often operating in a small data regime. The acquisition of sleep data is a substantial investment; therefore, any reduction in the data required for decoding has a profound impact. Furthermore, building upon the foundation of existing offline decoding, we initially developed a real-time staging model whose performance rivals that of offline staging algorithms. Subsequently, we refined the preprocessing pipeline to enable real-time decoding based on the established model structure, thus completing a closed-loop real-time sleep monitoring system. Our real-time sleep staging and decoding model present a robust tool for manipulating memory reactivation in real-time during sleep, opening new avenues for cognitive research during sleep and facilitating closed-loop editing of content-specific memories. Moreover, given the similarities in high-temporal-resolution brain recordings, our model can be effectively adapted to MEG or sEEG applications.

ETHICS STATEMENT

The research that has been documented adheres to the ethical guidelines outlined by the ICLR. The data acquisition and the follow-up experiments were approved by the local ethics community in *anonymous organization* (ethics review ID: *ICBIR_A_0204_005*). Every participant signed an informed consent form, acknowledging their rights. Participants were compensated with cash.

REPRODUCIBILITY STATEMENT

Code to train models and reproduce the results was submitted as part of the supplementary materials.

REFERENCES

- Alexei Baevski, Yuhao Zhou, Abdelrahman Mohamed, and Michael Auli. wav2vec 2.0: A framework for self-supervised learning of speech representations. *Advances in neural information processing systems*, 33:12449–12460, 2020.
- Yunpeng Bai, Xintao Wang, Yanpei Cao, Yixiao Ge, Chun Yuan, and Ying Shan. Dreamdiffusion: Generating high-quality images from brain eeg signals. *arXiv preprint arXiv:2306.16934*, 2023.
- Tadas Baltrušaitis, Chaitanya Ahuja, and Louis-Philippe Morency. Multimodal machine learning: A survey and taxonomy. *IEEE transactions on pattern analysis and machine intelligence*, 41(2): 423–443, 2018.
- Svenja Brodt, Marion Inostroza, Niels Niethard, and Jan Born. Sleep—a brain-state serving systems memory consolidation. *Neuron*, 111(7):1050–1075, 2023.
- Ting Chen, Simon Kornblith, Mohammad Norouzi, and Geoffrey Hinton. A simple framework for contrastive learning of visual representations. In *International conference on machine learning*, pp. 1597–1607. PMLR, 2020.
- Zijiao Chen, Jiaxin Qing, Tiange Xiang, Wan Lin Yue, and Juan Helen Zhou. Seeing beyond the brain: Conditional diffusion model with sparse masked modeling for vision decoding. In *Proceedings of the IEEE/CVF Conference on Computer Vision and Pattern Recognition*, pp. 22710–22720, 2023.
- Alexandre Défossez, Charlotte Caucheteux, Jérémy Rapin, Ori Kabeli, and Jean-Rémi King. Decoding speech from non-invasive brain recordings. *arXiv preprint arXiv:2208.12266*, 2022.
- Jacob Devlin, Ming-Wei Chang, Kenton Lee, and Kristina Toutanova. Bert: Pre-training of deep bidirectional transformers for language understanding. *arXiv preprint arXiv:1810.04805*, 2018.
- Martin Dresler, Renate Wehrle, Victor I Spoormaker, Stefan P Koch, Florian Holsboer, Axel Steiger, Hellmuth Obrig, Philipp G Sämann, and Michael Czisch. Neural correlates of dream lucidity obtained from contrasting lucid versus non-lucid rem sleep: a combined eeg/fmri case study. *Sleep*, 35(7):1017–1020, 2012.
- Yaroslav Ganin, Evgeniya Ustinova, Hana Ajakan, Pascal Germain, Hugo Larochelle, François Laviolette, Mario Marchand, and Victor Lempitsky. Domain-adversarial training of neural networks. *The journal of machine learning research*, 17(1):2096–2030, 2016.
- Alexandre Gramfort, Martin Luessi, Eric Larson, Denis A Engemann, Daniel Strohmeier, Christian Brodbeck, Roman Goj, Mainak Jas, Teon Brooks, Lauri Parkkonen, et al. Meg and eeg data analysis with mne-python. *Frontiers in neuroscience*, pp. 267, 2013.
- James V Haxby, J Swaroop Guntupalli, Samuel A Nastase, and Ma Feilong. Hyperalignment: Modeling shared information encoded in idiosyncratic cortical topographies. *elife*, 9:e56601, 2020.
- Kaiming He, Xinlei Chen, Saining Xie, Yanghao Li, Piotr Dollár, and Ross Girshick. Masked autoencoders are scalable vision learners. In *Proceedings of the IEEE/CVF conference on computer vision and pattern recognition*, pp. 16000–16009, 2022.

-
- Tomoyasu Horikawa, Masako Tamaki, Yoichi Miyawaki, and Yukiyasu Kamitani. Neural decoding of visual imagery during sleep. *Science*, 340(6132):639–642, 2013.
- Lukas Hoyer, Dengxin Dai, and Luc Van Gool. Daformer: Improving network architectures and training strategies for domain-adaptive semantic segmentation. In *Proceedings of the IEEE/CVF Conference on Computer Vision and Pattern Recognition*, pp. 9924–9935, 2022.
- Xiaoqing Hu, Larry Y Cheng, Man Hey Chiu, and Ken A Paller. Promoting memory consolidation during sleep: A meta-analysis of targeted memory reactivation. *Psychological bulletin*, 146(3): 218, 2020.
- Elias B Issa and Xiaoqin Wang. Altered neural responses to sounds in primate primary auditory cortex during slow-wave sleep. *Journal of Neuroscience*, 31(8):2965–2973, 2011.
- Prannay Khosla, Piotr Teterwak, Chen Wang, Aaron Sarna, Yonglong Tian, Phillip Isola, Aaron Maschinot, Ce Liu, and Dilip Krishnan. Supervised contrastive learning. *Advances in neural information processing systems*, 33:18661–18673, 2020.
- Donghyun Kim, Yi-Hsuan Tsai, Bingbing Zhuang, Xiang Yu, Stan Sclaroff, Kate Saenko, and Manmohan Chandraker. Learning cross-modal contrastive features for video domain adaptation. In *Proceedings of the IEEE/CVF International Conference on Computer Vision*, pp. 13618–13627, 2021.
- Jens G Klinzing, Niels Niethard, and Jan Born. Mechanisms of systems memory consolidation during sleep. *Nature neuroscience*, 22(10):1598–1610, 2019.
- Karen R Konkoly, Kristoffer Appel, Emma Chabani, Anastasia Mangiaruga, Jarrod Gott, Remington Mallett, Bruce Caughran, Sarah Witkowski, Nathan W Whitmore, Christopher Y Mazurek, et al. Real-time dialogue between experimenters and dreamers during rem sleep. *Current Biology*, 31(7):1417–1427, 2021.
- Demetres Kostas, Stephane Aroca-Ouellette, and Frank Rudzicz. Bendr: using transformers and a contrastive self-supervised learning task to learn from massive amounts of eeg data. *Frontiers in Human Neuroscience*, 15:653659, 2021.
- Sid Kouider, Thomas Andrillon, Leonardo S Barbosa, Louise Goupil, and Tristan A Bekinschtein. Inducing task-relevant responses to speech in the sleeping brain. *Current Biology*, 24(18):2208–2214, 2014.
- Alex Krizhevsky, Ilya Sutskever, and Geoffrey E Hinton. Imagenet classification with deep convolutional neural networks. *Advances in neural information processing systems*, 25, 2012.
- Adam Li, Jacob Feitelberg, Anand Prakash Saini, Richard Höchenberger, and Mathieu Scheltienne. Mne-icalabel: Automatically annotating ica components with iclabel in python. *Journal of Open Source Software*, 7(76):4484, 2022a.
- Rui Li, Yiting Wang, Wei-Long Zheng, and Bao-Liang Lu. A multi-view spectral-spatial-temporal masked autoencoder for decoding emotions with self-supervised learning. In *Proceedings of the 30th ACM International Conference on Multimedia*, pp. 6–14, 2022b.
- Yunzhe Liu, Raymond J Dolan, Cameron Higgins, Hector Penagos, Mark W Woolrich, H Freyja Ólafsdóttir, Caswell Barry, Zeb Kurth-Nelson, and Timothy E Behrens. Temporally delayed linear modelling (tdlm) measures replay in both animals and humans. *Elife*, 10:e66917, 2021.
- Yunzhe Liu, Matthew M Nour, Nicolas W Schuck, Timothy EJ Behrens, and Raymond J Dolan. Decoding cognition from spontaneous neural activity. *Nature Reviews Neuroscience*, 23(4):204–214, 2022.
- Hong-Viet V Ngo and Bernhard P Staresina. Shaping overnight consolidation via slow-oscillation closed-loop targeted memory reactivation. *Proceedings of the National Academy of Sciences*, 119(44):e2123428119, 2022.
- Mehdi Noroozi and Paolo Favaro. Unsupervised learning of visual representations by solving jigsaw puzzles. In *European conference on computer vision*, pp. 69–84. Springer, 2016.

-
- Deepak Pathak, Philipp Krahenbuhl, Jeff Donahue, Trevor Darrell, and Alexei A Efros. Context encoders: Feature learning by inpainting. In *Proceedings of the IEEE conference on computer vision and pattern recognition*, pp. 2536–2544, 2016.
- Minlong Peng, Qi Zhang, Yu-gang Jiang, and Xuan-Jing Huang. Cross-domain sentiment classification with target domain specific information. In *Proceedings of the 56th Annual Meeting of the Association for Computational Linguistics (Volume 1: Long Papers)*, pp. 2505–2513, 2018.
- Alec Radford, Jong Wook Kim, Chris Hallacy, Aditya Ramesh, Gabriel Goh, Sandhini Agarwal, Girish Sastry, Amanda Askell, Pamela Mishkin, Jack Clark, et al. Learning transferable visual models from natural language supervision. In *International conference on machine learning*, pp. 8748–8763. PMLR, 2021.
- Björn Rasch, Christian Büchel, Steffen Gais, and Jan Born. Odor cues during slow-wave sleep prompt declarative memory consolidation. *Science*, 2007.
- Monika Schönauer, Sarah Alizadeh, Hamidreza Jamalabadi, Annette Abraham, Annedore Pawlizki, and Steffen Gais. Decoding material-specific memory reprocessing during sleep in humans. *Nature Communications*, 8(1):15404, 2017.
- Thomas Schreiner, Marit Petzka, Tobias Staudigl, and Bernhard P Staresina. Endogenous memory reactivation during sleep in humans is clocked by slow oscillation-spindle complexes. *Nature communications*, 12(1):3112, 2021.
- Francesca Siclari, Benjamin Baird, Lampros Perogamvros, Giulio Bernardi, Joshua J LaRocque, Brady Riedner, Melanie Boly, Bradley R Postle, and Giulio Tononi. The neural correlates of dreaming. *Nature neuroscience*, 20(6):872–878, 2017.
- William E Skaggs and Bruce L McNaughton. Replay of neuronal firing sequences in rat hippocampus during sleep following spatial experience. *Science*, 271(5257):1870–1873, 1996.
- Melanie Strauss, Jacobo D Sitt, Jean-Remi King, Maxime Elbaz, Leila Azizi, Marco Buiatti, Lionel Naccache, Virginie Van Wassenhove, and Stanislas Dehaene. Disruption of hierarchical predictive coding during sleep. *Proceedings of the National Academy of Sciences*, 112(11):E1353–E1362, 2015.
- Mingyi Sun, Weigang Cui, Shuyue Yu, Hongbin Han, Bin Hu, and Yang Li. A dual-branch dynamic graph convolution based adaptive transformer feature fusion network for eeg emotion recognition. *IEEE Transactions on Affective Computing*, 13(4):2218–2228, 2022.
- Başak Türker, Esteban Munoz Musat, Emma Chabani, Alexandrine Fonteix-Galet, Jean-Baptiste Maranci, Nicolas Wattiez, Pierre Pouget, Jacobo Sitt, Lionel Naccache, Isabelle Arnulf, et al. Behavioral and brain responses to verbal stimuli reveal transient periods of cognitive integration of external world in all sleep stages. *bioRxiv*, pp. 2022–05, 2022.
- Raphael Vallat and Matthew P Walker. An open-source, high-performance tool for automated sleep staging. *Elife*, 10:e70092, 2021a.
- Raphael Vallat and Matthew P Walker. An open-source, high-performance tool for automated sleep staging. *eLife*, 10:e70092, oct 2021b. ISSN 2050-084X. doi: 10.7554/eLife.70092. URL <https://doi.org/10.7554/eLife.70092>.
- Jindong Wang, Cuiling Lan, Chang Liu, Yidong Ouyang, Tao Qin, Wang Lu, Yiqiang Chen, Wenjun Zeng, and Philip Yu. Generalizing to unseen domains: A survey on domain generalization. *IEEE Transactions on Knowledge and Data Engineering*, 2022a.
- Rui Wang, Zuxuan Wu, Zejia Weng, Jingjing Chen, Guo-Jun Qi, and Yu-Gang Jiang. Cross-domain contrastive learning for unsupervised domain adaptation. *IEEE Transactions on Multimedia*, 2022b.
- Matthew A Wilson and Bruce L McNaughton. Reactivation of hippocampal ensemble memories during sleep. *Science*, 265(5172):676–679, 1994.

-
- Dezhong Yao. A method to standardize a reference of scalp eeg recordings to a point at infinity. *Physiological measurement*, 22(4):693, 2001.
- Richard Zhang, Phillip Isola, and Alexei A Efros. Colorful image colorization. In *Computer Vision—ECCV 2016: 14th European Conference, Amsterdam, The Netherlands, October 11-14, 2016, Proceedings, Part III 14*, pp. 649–666. Springer, 2016.
- Li-Ming Zhao, Xu Yan, and Bao-Liang Lu. Plug-and-play domain adaptation for cross-subject eeg-based emotion recognition. In *Proceedings of the AAAI Conference on Artificial Intelligence*, pp. 863–870, 2021.
- Yongchun Zhu, Fuzhen Zhuang, Jindong Wang, Guolin Ke, Jingwu Chen, Jiang Bian, Hui Xiong, and Qing He. Deep subdomain adaptation network for image classification. *IEEE transactions on neural networks and learning systems*, 32(4):1713–1722, 2020.

A EXPERIMENT DESIGN

As demonstrated in Fig.1, our experiment paradigm contained three stages: pre-sleep function localizer stage, overnight sleep target memory reactivation stage, and post-sleep function localizer stage. First, we selected 15 semantic classes: alarm, apple, ball, book, box, chair, kiwi, microphone, motorcycle, pepper, sheep, shoes, strawberry, tomato, watch. Then, we used the corresponding pictures and sounds to form the image-set (i.e., containing 15 different pictures) and the audio-set (i.e., containing 15 different sounds). It's worth noting that the sound corresponding to the picture can easily trigger the recall of the associated picture, e.g., the picture of "sheep" is paired with the sound of the "sheep" instead of other unrelated sounds.

A.1 PRE&POST-SLEEP FUNCTION LOCALIZER STAGE

In the pre-sleep function localizer stage, the subject was instructed to perform two tasks: the image-audio task and the audio-image task. In image-audio task, the subject was presented with 600 trials, with each trial containing one picture and one sound, in image-audio order. We randomly selected one picture and one sound from image-set and audio-set respectively, to form an image-audio pair. In each image-audio pair, the picture and the sound may be inconsistent. In total, we had 210 inconsistent trials and 390 consistent trials. The "consistent trial" means the sound and the picture in that trial belong to the same stimulus pair, and the "inconsistent trial" means the sound and the picture in that trial don't belong to the same stimulus pair. The purpose of this design is solely to confirm that participants had formed correct and stable stimulus pair memories.

For each trial, the subject was presented with the following items in sequence:

- a blank screen for 0.6s-0.9s (i.e., inter-trial interval),
- a cross centered at the screen for 0.3s,
- an image cue of that image-audio pair for 0.8s,
- a blank screen for 0.3s,
- an audio cue of that image-audio pair for 0.5s,
- a blank screen for 0.3s.

Then, the subject was required to decide whether the presented image cue and audio cue are matched. Finally, we presented the behavior feedback for 0.2s. In total, image-audio task took about 48 minutes.

The setup of audio-image task was similar to that of image-audio task. In audio-image task, the only difference from image-audio task was that we presented image-audio pairs in audio-image order.

In the post-sleep function localizer stage, the subject was required to execute the same tasks in the pre-sleep function localizer stage.

A.2 OVERNIGHT SLEEP TARGET MEMORY REACTIVATION STAGE

In the overnight sleep target memory reactivation stage, we utilized a closed-loop stimulation system that allows for real-time, automatic sleep staging. As the subject reached the N2/3 stage of NREM sleep, the subject was presented with audio cues (which are the same as those during wakefulness, each lasting 0.5s), randomly selected from audio-set, every 4-6 seconds. This approach provided clear timing and content of memory reactivation during sleep, aiding in the training of a neural decoder on these cued sleep intervals.

A.3 DATASET SUMMARY

In total, we collect datasets from 134 subjects (122 subjects from one laboratory, 12 subjects from another laboratory). This operation is to better demonstrate the generalization ability of our model.

B PREPROCESSING

EEG signals are filtered within the frequency range of 0.1-50Hz. Line noise at 50Hz and its harmonics are removed. Each channel is re-referenced by subtracting out the mean signal over all EEG channels (average re-referencing). This decreases the effect caused by online-reference channel selection (Yao, 2001). Then we apply Independent Component Analysis (ICA) and remove artifact components automatically (Li et al., 2022a). The preprocessed EEG signals are further resampled to 100Hz. Finally, we epoch the EEG signals from -0.2s to 0.8s for awake EEG signals and from -0.2s to 1.8s for sleep EEG signals according to the onset of the stimuli cue (e.g. image, audio), and drop noisy epochs automatically. All of the above operations are done with MNE-Python (Gramfort et al., 2013).

The preprocess pipeline of sleep data contains one more step, i.e., sleep staging, at the very beginning. To this aim, we follow the standard pipeline of YASA-Python (Vallat & Walker, 2021a). According to the recommendation of the algorithm, we provide a central electrode *C3* referenced to the mastoid *M2* (i.e., $C3 - M2$) as the EEG channel, the right EOG channel *REOG* referenced to the mastoid *M2* (i.e., $REOG - M2$) as the EOG channel, and the right EMG channel *REMG* referenced to the reference EMG channel *EMGREF* (i.e., $REMG - EMGREF$) as the EMG channel. After the sleep staging, we truncate EEG signals according to NREM 2/3 sleep stage, and splice them together in sequence to form the TMR-related EEG signals of that subject.

C MODEL PARAMETERS

The configuration of the USD model for N2/3 state training is listed in Table.1 and the configuration of the USD model for REM state training is listed in Table.2.

For the pretraining of both models, each model is trained up to 500 epochs by default using Adam with a learning rate of $2 \cdot 10^{-5}$. For the fine-tuning of these models, we freeze all the Conv1D layers in the encoders. Then, each model is fine-tuned up to 200 epochs by default using Adam with a learning rate of $1 \cdot 10^{-5}$.

The pretraining and fine-tuning of both models were done with a batch size of 256 on one NVIDIA V100 GPU with 32GB of memory.

C.1 UNIVERSAL SLEEP DECODER FOR N2/3 PARAMETERS

C.2 UNIVERSAL SLEEP DECODER FOR REM PARAMETERS

Table 1: The configuration of Universal Sleep Decoder for N2/3 training setting

blocks	layers	d_{hidden}^1	n_{head}^2	d_{head}^3	other parameters
Sleep Encoder	Conv1D	256	-	-	$(k,d,s)^4 = (9,1,1)$
	Conv1D	256	-	-	$(k,d,s) = (9,2,1)$
	Conv1D	256	-	-	$(k,d,s) = (9,4,1)$
	Conv1D	256	-	-	$(k,d,s) = (9,1,1)$
	Conv1D	256	-	-	$(k,d,s) = (9,2,1)$
	Conv1D	256	-	-	$(k,d,s) = (9,4,1)$
	Dropout	rate = 0.3	-	-	-
	BatchNorm	-	-	-	-
	Linear	256	-	-	-
	Linear	128	-	-	-
	Attention $\times 12$		1024	6	64
Awake Encoder	Conv1D	256	-	-	$(k,d,s) = (9,1,1)$
	Conv1D	256	-	-	$(k,d,s) = (9,2,1)$
	Conv1D	256	-	-	$(k,d,s) = (9,4,1)$
	Conv1D	256	-	-	$(k,d,s) = (9,1,1)$
	Conv1D	256	-	-	$(k,d,s) = (9,2,1)$
	Conv1D	256	-	-	$(k,d,s) = (9,4,1)$
	Dropout	rate = 0.3	-	-	-
	BatchNorm	-	-	-	-
	Linear	256	-	-	-
	Linear	128	-	-	-
Shared Image-Sleep Encoder	Attention $\times 4$	1024	4	64	$dropout_{ff} = [0.5, 0.5]$
	BatchNorm	-	-	-	-
Shared Audio-Sleep Encoder	Attention $\times 6$	1024	6	64	$dropout_{ff} = [0.5, 0.5]$
	BatchNorm	-	-	-	-
Sleep Feature	Linear	256	-	-	-
Image Feature	Linear	256	-	-	-
Audio Feature	Linear	256	-	-	-
Image-Audio Contrastive	Linear	$[64, 64]^6$	-	-	-
	Flatten	\checkmark^7	-	-	-
Sleep-Image Contrastive	Linear	$[32, 80]$	-	-	-
	Flatten	\checkmark	-	-	-
Sleep-Audio Contrastive	Linear	$[32, 80]$	-	-	-
	Flatten	-	-	-	-
Sleep Classification	Flatten	-	-	-	-
	Linear	128	-	-	-
	Linear	15	-	-	-
Image Classification	Flatten	-	-	-	-
	Linear	128	-	-	-
	Linear	15	-	-	-
Audio Classification	Flatten	-	-	-	-
	Linear	128	-	-	-
	Linear	15	-	-	-

¹ d_{hidden} refers to the dimensions of the hidden layer in Feed Forward Network.² n_{head} refers to the number of attention heads.³ d_{head} refers to the dimensions of attention head.⁴ (k,d,s) refers to the (kernel size, dilation rate, stride) in Convolutional Network.⁵ $dropout_{ff}$ refers to the dropout probability of the hidden layer in Feed Forward Network.⁶ The numbers correspond sequentially to the parameters of the linear layers for contrastive learning items.

Table 2: The configuration of Universal Sleep Decoder for REM training setting

blocks	layers	d_{hidden}^1	n_{head}^2	d_{head}^3	other parameters
Sleep Encoder	Conv1D	256	-	-	(k,d,s) ⁴ = (9,1,1)
	Conv1D	256	-	-	(k,d,s) = (9,2,1)
	Dropout	rate = 0.3	-	-	-
	BatchNorm	-	-	-	-
	Linear	256	-	-	-
	Linear	128	-	-	-
	Attention × 12	1024	6	64	$dropout_{ff}^5 = [0.5, 0.5]$
Awake Encoder	Conv1D	256	-	-	(k,d,s) = (9,1,1)
	Conv1D	256	-	-	(k,d,s) = (9,2,1)
	Dropout	rate = 0.3	-	-	-
	BatchNorm	-	-	-	-
	Linear	256	-	-	-
	Linear	128	-	-	-
	Subject Layer	-	-	-	-
Shared Image-Sleep Encoder	Attention × 4	1024	4	64	$dropout_{ff} = [0.5, 0.5]$
	BatchNorm	-	-	-	-
Shared Audio-Sleep Encoder	Attention × 6	1024	6	64	$dropout_{ff} = [0.5, 0.5]$
	BatchNorm	-	-	-	-
Sleep Feature	Linear	256	-	-	-
Image Feature	Linear	256	-	-	-
Audio Feature	Linear	256	-	-	-
Image-Audio Contrastive	Linear	$[64, 64]^6$	-	-	-
	Flatten	✓ ⁷	-	-	-
Sleep-Image Contrastive	Linear	$[32, 80]$	-	-	-
	Flatten	✓	-	-	-
Sleep-Audio Contrastive	Linear	$[32, 80]$	-	-	-
	Flatten	-	-	-	-
Sleep Classification	Flatten	-	-	-	-
	Linear	128	-	-	-
	Linear	15	-	-	-
Image Classification	Flatten	-	-	-	-
	Linear	128	-	-	-
	Linear	15	-	-	-
Audio Classification	Flatten	-	-	-	-
	Linear	128	-	-	-
	Linear	15	-	-	-

¹ d_{hidden} refers to the dimensions of the hidden layer in Feed Forward Network.

² n_{head} refers to the number of attention heads.

³ d_{head} refers to the dimensions of attention head.

⁴ (k,d,s) refers to the (kernel size, dilation rate, stride) in Convolutional Network.

⁵ $dropout_{ff}$ refers to the dropout probability of the hidden layer in Feed Forward Network.

⁶ The two numbers in square brackets correspond to the parameters of the corresponding linear layers of the first and second terms of contrastive learning.